

EROSION OF A COPPER CATHODE IN A NONSTATIONARY ARC SPOT. II. DETERMINATION OF THE ENERGY PARAMETERS OF THE ARC SPOT BY THE THERMOPHYSICAL METHOD

L. I. Sharakhovskii,^a A. M. Esipchuk,^{a,b}
and A. Marotta^b

UDC 621.387.143.014.31

The results of investigation of the energy parameters of a nonstationary electric-arc spot on a copper cathode in an air atmosphere have been presented. The data published earlier on the thermal volt-equivalent of the cathode arc spot have been generalized. A nonlinear dependence of the current density on the magnetic field has been obtained. A comparison of the new results and those obtained earlier on other setups and their generalization have been made.

Investigation. The results of experiments on investigation of the basic regularities of the erosion of a copper cathode in an arc spot moving under the action of a magnetic field have been presented in [1]. To better understand these results and to interpret them physically from a unified standpoint one can employ the thermal macroscopic model of erosion of cold electrodes of [2, 3]. In it, the erosion is considered as the process of thermal ablation of the electrode material under the action of an intense heat flux in an arc spot, where the density q_0 is determined by the current density j and the thermal volt-equivalent U , i.e.,

$$q_0 = jU. \quad (1)$$

This expression immediately follows from the determination of the thermal equivalent of the arc spot $U \equiv Q_0/I = q_0 F/I$ [2–5]. Thus, the most important energy parameters determining the service life and erosion of an electrode are the current density and the thermal volt-equivalent, whose behavior with change in the magnetic field is the subject of investigation of the present work.

As has been found in experiments in which modern optico-electronic equipment with a high temporal and spatial resolution was used, the physical processes in the arc spot on a cold cathode are not stationary even without its movement by a magnetic field. The spot has a very complex and dynamic internal structure consisting of numerous mobile, short-lived microspots separated in space. With advances in the recording technique, one finds increasingly smaller details of the complex hierarchical microstructure of a cathode spot. This makes it very difficult and ambiguous to determine the dimensions of the conductive zone (diameter of the spot d), which directly influences the value of the current density if it is determined by the traditional method, by employing the values of the current I and the spot diameter according to the relation $j = 4I/\pi d^2$.

The thermal model of an arc spot enables us to circumvent these difficulties by introducing the concept of effective current density. To obtain the latter we must record the surface temperature of the electrode and the velocity of movement of the arc at the instant of the beginning of fusion on a macroscopic scale. Without measuring the arc diameter directly, we can calculate with this method the value of the current density, instrumentally averaged by the thermal effect, according to the relation [6]

^aA. V. Luikov Heat and Mass Transfer Institute, National Academy of Sciences of Belarus, 15 P. Brovka Str., Minsk, 220072, Belarus; email: leonidsh@tut.by; ^bGleb Wataghin Institute of Physics, Campinas State University, Campinas, Brazil (Instituto de Fisica "Gleb Wataghin", Universidade Estadual de Campinas, Campinas, São Paulo, Brasil); email: aruy@ifi.unicamp.br. Translated from *Inzhenerno-Fizicheskii Zhurnal*, Vol. 77, No. 2, pp. 112–117, March–April, 2004. Original article submitted October 13, 2003.

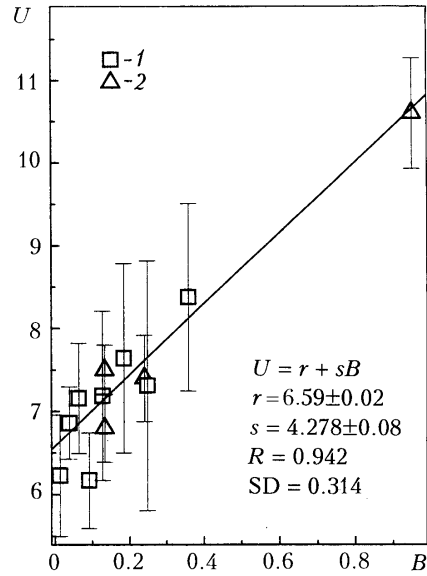


Fig. 1. Thermal volt-equivalent U of the arc spot on the copper cathode as a function of the magnetic induction B . The results of the experiments: 1) on the GWIP setup; 2) on the HMTI setup.

$$j = \frac{\pi}{4} \left[\frac{\lambda^2 v}{an \sqrt{I}} \left(\frac{T_f - T_0}{U} \right)^2 \right]^{2/3}, \quad (2)$$

if the thermal volt-equivalent U is measured by an independent method. Such an effective value of the current density can be directly employed in thermal calculations of the electrodes as the macroscopic characteristic of the spot.

In formula (2), T_0 is the temperature of the surface immediately ahead of the incident spot. Owing to the small dimensions of the spot and the short duration of its action as compared to the time of cooling between the periods of arrival at a given point, this temperature differs only slightly from the average temperature of the electrode surface. One can obtain it by simple measurement with a thermocouple on a fixed radius of an orificed electrode with simultaneous measurement of the average density of the heat flux into the electrode [7]. The average velocity of the arc spot v can easily be obtained, for example, by measuring the velocity of rotation of the arc about the circle of the electrodes. The parameter $n = L/d$ enables us to allow for the character of motion of the spot — continuous or discontinuous (with stops). For continuous motion we take $n = 1$ [6].

Description of the Procedure. In the present work, to obtain the effective current density we have employed the results obtained on a setup for investigation of erosion in a stationary thermal regime and described in the first part of the work. The stationary procedure of determination of the current density lay in applying the assumption that transition from micro- to macroerosion corresponds to the beginning of macrofusion in the spot to erosion experiments. Then, measuring the surface temperature T_0 , the spot velocity v , and the current density I at the instant of the beginning of erosion, we can obtain the effective current density from relation (2) if we measure U and n in advance by independent methods.

To obtain the value of the thermal volt-equivalent U we must determine the heat flux through the arc spot (measurement of the thermal volt-equivalent in the case of rapidly moving spots presents certain difficulties). Calorimetric methods used under nonstationary conditions of heating of the electrode enable one to indirectly separate from the total heat flux that part of it which arrives through the arc spot. The variants of the procedure of measurement of U have been described in [4, 6, 8] in detail. Here we have employed all the earlier results, which were subjected to combined additional processing with the aim of generalizing and systematizing; the results of the processing are shown in Fig. 1. Experimental results (more than 360 experimental points) obtained with the use of different procedures can be approximated by the linear function of the magnetic field

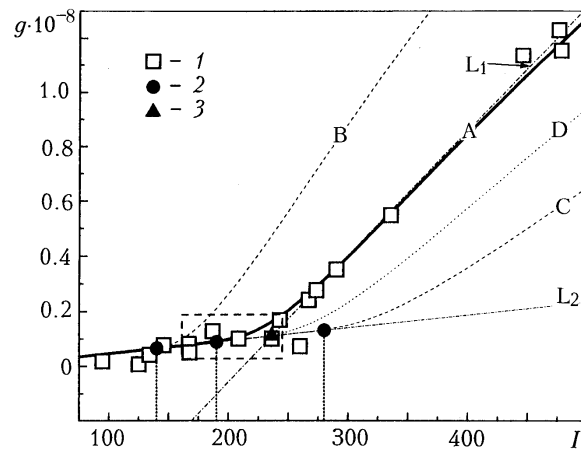


Fig. 2. Behavior of the specific erosion g as a function of the current I ($B = 0.137$ T) and modeling of the specific erosion for determination of the effective current density: 1) experimental points; 2 and 3) critical points. The theoretical curves for $h_{\text{eff}} = 33 \text{ MJ}\cdot\text{kg}^{-1}$ are: A, B, and C for $j = 2.08\cdot 10^9$, $2.28\cdot 10^9$, and $1.88\cdot 10^9 \text{ A}\cdot\text{m}^{-2}$; L_1 and L_2 , linear approximations for macro- and microerosion; D, $j = 1.98\cdot 10^9 \text{ A}\cdot\text{m}^{-2}$. In the dashed frame are the points employed for calculation of the current density by the averaging method (see the text and Figs. 4, 5, and 6 for details).

$$U = r + sB. \quad (3)$$

Here $r = (6.59 \pm 0.02) \text{ V}$, i.e., the deviation is 0.3%, and $s = (4.28 \pm 0.08) \text{ V/T}$, i.e., the deviation is 2%. The correlation coefficient is equal to 0.94 with a variance of 0.314. The expression obtained was employed in further calculations of the current density in the arc spot.

As far as the parameter n is concerned, since we did not measure the length of the arc-spot step, we could determine only the apparent current density, which was obtained under the assumption that $n = 1$ and which was equal to the real density only in the case of continuous motion of the spot or step motion in the particular case with $L = d$. Measurement of n requires sophisticated optical equipment with a very high spatial and temporal resolution, since the step of the spot for determination of n must be measured to an accuracy no less than the spot diameter d . This diameter is as small as about 1 mm even for a current of 1 kA [4]. For a velocity of the spot of $100 \text{ m}\cdot\text{sec}^{-1}$ the attainment of the prescribed accuracy requires a frequency of recording of the position of the spot of the order of 10^5 frames per second with a considerable total number of frames, since for reliable data to be obtained they must be processed statistically in the case of nonuniform motion of the spot.

The idea of a stationary method of determination of the current density is clearly seen from Fig. 3A [1], where micro- and macroerosion are approximated by simple linear current functions. Thus, the condition $f = 1$ is observed in this figure at points 5 corresponding to the transition from micro- to macroerosion. Knowledge of the temperature of the electrode surface T_0 , the velocity of movement of the spot v , and the current density I at these points enables us, using relation (2), to compute the value of j corresponding to the stationary conditions. This figure can be considered as a simplified pictorial scheme for illustration of the stationary thermal procedure of determination of the current density. From the thermal model it follows that the specific erosion in the macroerosion regime is not a linear current function and the transition from micro- to macroerosion on the graph $g(I)$ is of smooth nonlinear character. The specific erosion [2, 3]

$$g = g_0 + \frac{UW}{h_{\text{eff}}} \quad (4)$$

is determined by the dimensionless erosion energy W

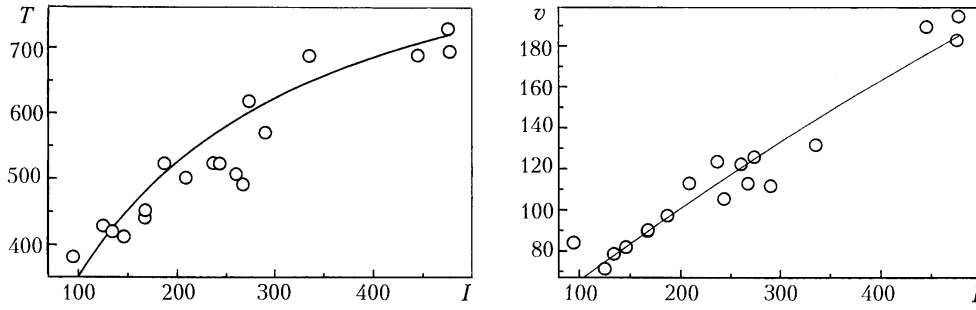


Fig. 3. Nonlinear approximations of the experimental dependences of the electrode temperature T and the velocity of movement of the arc spot v on the current I in the form of the rational functions $v = a_1 - b_1/(I + c_1)$ and $T = a_2 - b_2/(I + c_2)$, employed in modeling the theoretical curves of specific erosion as a function of the current $g(I)$ in Fig. 2 from Eqs. (4)–(7). Here $a_1 = 941.32$; $b_1 = 2.092 \cdot 10^6$; $c_1 = 2289$; $a_2 = 692.75$; $b_2 = 155.14 \cdot 10^3$; $c_2 = 152.61$. T , °C; v , m·sec⁻¹; I , A.

$$W \approx 1 - f \left(\frac{7.13}{2.475 + f} + \frac{0.442}{0.04 + f} - 1.477 \right), \quad (5)$$

which nonlinearly depends on the dimensionless parameter of fusion in the arc spot f

$$f = \frac{\pi^{1.5} v \lambda^2 (T_f - T_0)^2}{8 a_j^{1.5} U^2 I^{0.5} n}, \quad (6)$$

including some dimensional parameters.

To construct the theoretical dependence $g(I)$ we must know the real dependence of the parameter $f(I)$, which can be found from (6) with the use of the empirical dependences $T(I)$ and $v(I)$ obtained from the same experiments. In addition to the current density j , the unknowns appearing in (4)–(6) are the effective enthalpy of erosion h_{eff} and the parameter of motion n , which has been taken to be $n = 1$ under the assumption of continuous motion in the present investigations. Strictly speaking, the value of the effective erosion enthalpy h_{eff} does not influence determination of the point of transition from micro- to macroerosion, since the rate of growth of the erosion depends on it only after the transition to macroerosion.

In [1], it has been shown that the specific microerosion has a tendency toward growth with current and does not have a rigorous constant value, and it can be approximated by a linear function. In processing the experiments, we employed the dependence for the microerosion g_0 :

$$g_0 = 4.68 \cdot 10^{-12} I. \quad (7)$$

Figure 2 illustrates the stationary procedure of obtaining the current density with the example of erosion experiments conducted for a magnetic induction of 0.317 T. The solid curve A shows the theoretical dependence $g(I)$ calculated in accordance with (4)–(7) for the current density $j = 2.08 \cdot 10^9$ A·m⁻² and the effective enthalpy $h_{\text{eff}} = 33$ MJ·kg⁻¹. In the calculation, we have employed the empirical nonlinear approximations of $T(I)$ and $v(I)$ (shown in Fig. 3) of the data obtained in this set of experiments.

The dashed curves B and C in Fig. 2 show the theoretical dependences for the same value of the enthalpy $h_{\text{eff}} = 33$ MJ·kg⁻¹ but for the current densities $j = 2.08 \pm 0.2 \cdot 10^9$ A·m⁻² corresponding to a 10% change in the direction of increasing or decreasing values. It is clear that the correspondence to experiment has been obtained for $j = 2.08 \cdot 10^9$ A·m⁻², which was taken for the given magnetic field in further processing of the experiments. It should be noted that the change in j substantially influences the position of the critical points 2.

The linear approximations of macro- and microerosion are shown as the straight lines L_1 and L_2 respectively in Fig. 2; they yield the critical point 3 shifted to the region of higher currents. The theoretical curve D for the critical

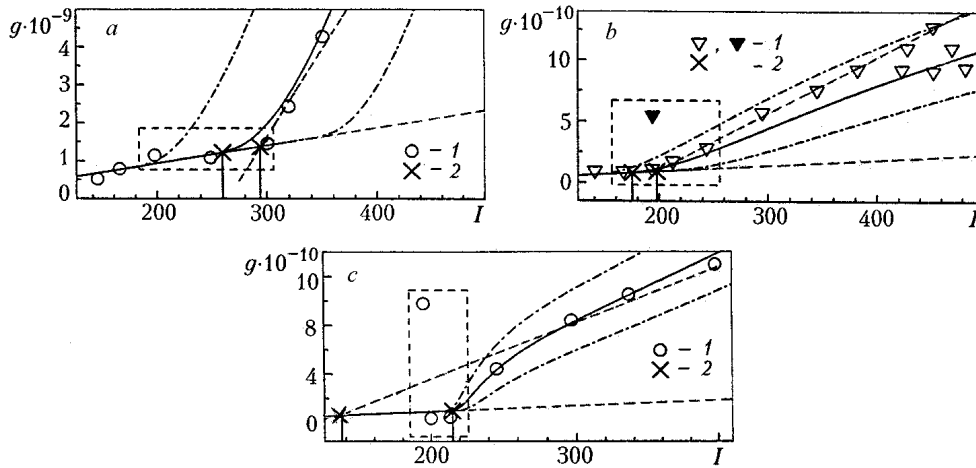


Fig. 4. Modeling of the dependence of the specific erosion g as a function of the current I for different magnetic fields: a) $B = 0.01$; b) 0.2 ; c) 0.35 T. Solid curves: a) $j = 0.73 \cdot 10^9 \text{ A} \cdot \text{m}^{-2}$ and $h_{\text{eff}} = 45 \text{ MJ} \cdot \text{kg}^{-1}$; b) $j = 2.0 \cdot 10^9 \text{ A} \cdot \text{m}^{-2}$ and $h_{\text{eff}} = 35 \text{ MJ} \cdot \text{kg}^{-1}$; c) $j = 2.6 \cdot 10^9 \text{ A} \cdot \text{m}^{-2}$ and $h_{\text{eff}} = 33 \text{ MJ} \cdot \text{kg}^{-1}$; dashed straight lines: linear approximations of macro- and microerosion; dot-dash curves, variations of g with a change of $\pm 0.1 \cdot 10^9 \text{ A} \cdot \text{m}^{-2}$ in j ; 1) experimental points, the black point in Fig. 6 has been recorded at an elevated cathode temperature (see Fig. 5 for details); 2) critical points; in the dashed frame are the points employed for calculation of the current density by the averaging method (see the text and Figs. 2, 5, and 6 for details).

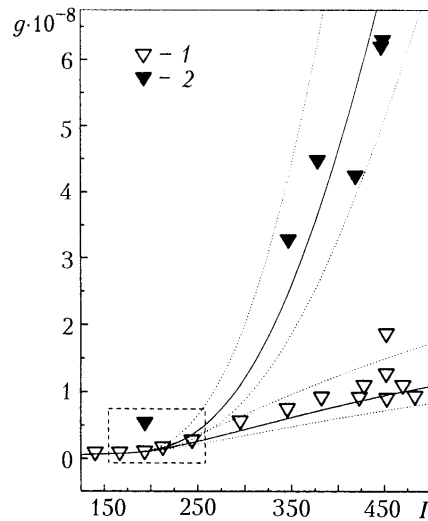


Fig. 5. Theoretical modeling of the experimental dependences $g(I)$ obtained for different thermal regimes of the cathode when $B = 0.2$ T: 1) thickness of the cooled wall 10 mm , normal cathode temperature; 2) thickness 40 mm , elevated cathode temperature. Solid curves: calculation for $j = 2.0 \cdot 10^9 \text{ A} \cdot \text{m}^{-2}$ and $h_{\text{eff}} = 35 \text{ MJ} \cdot \text{kg}^{-1}$; dotted curves, variation of the erosion with a change of $\pm 15 \text{ MJ} \cdot \text{kg}^{-1}$ in h_{eff} ; in the dashed frame are the points employed for calculation of the current density by the averaging method (see the text and Figs. 2, 4, and 6 for details).

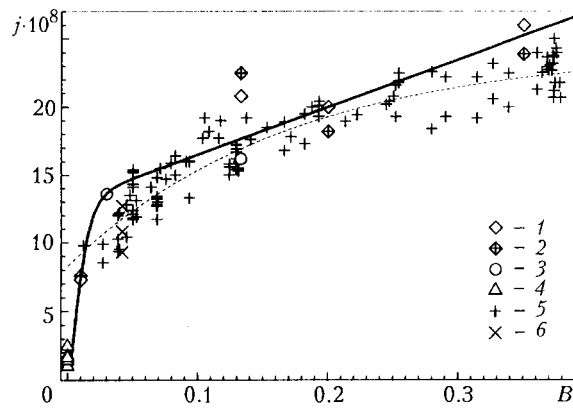


Fig. 6. Effective current density j vs. magnetic induction B : 1) results of the present work; 2) averaging method (see the text and Figs. 2, 4, and 5 for details); 3) modeling from [5]; 4) electrical measurements for $B = 0$ [9]; 5) nonstationary experiments [10]; 6) the same from [4]. Solid curve, approximation of points 1–4, formula (9); dotted curve, approximation of the results of the nonstationary experiments, formula (8).

point 3 is shifted from the experimental points and curve A and yields a value of the current density of $j = 1.98 \cdot 10^9 \text{ A}\cdot\text{m}^{-2}$, understated by $0.1 \cdot 10^9 \text{ A}\cdot\text{m}^{-2}$.

Figure 3 is an example of the empirical approximations of the experimental dependences $T(I)$ and $v(I)$ employed in constructing all the theoretical curves in Fig. 2. The nonlinear approximations of $T(I)$ and $v(I)$, which reproduced all the erosion fluctuations in the experiment best, were used for the closest modeling of the experimental function $g(I)$.

By the analogous modeling of erosion, we have determined the effective current density for other magnetic fields. Figure 4 shows experimental data on $g(I)$ and the results of modeling them with the thermal model for the other three magnetic fields (0.01, 0.2, and 0.35 T), whereas Fig. 5 shows the results for the same magnetic field ($B = 0.2 \text{ T}$) in two strongly differing thermal regimes of the cathode surface, which have been obtained by changing the thickness of the cooled wall. Points 1 correspond to a thickness of the cooled wall of 10 mm, and points 2 correspond to a thickness of 40 mm. It is seen that the model makes it possible to quite satisfactorily model the results of the experiments for all the regimes in Figs. 2–5. A change in the theoretical curve with a variation of $15 \text{ MJ}\cdot\text{kg}^{-1}$ in the effective enthalpy in the direction of increasing and decreasing values is shown in Fig. 5 as the dotted curves. It is clear that the effective enthalpy determines only the angular rotation of the theoretical curve about the experimental points and does not influence the position of the critical point of transition from micro- to macroerosion.

We can also calculate the average current density from the parameters of the $g(I)$ experimental points taken in the zone of sharp increase of the erosion, assuming that the condition $f = 1$ is observed at each of these points. In Figs. 2, 4, and 5 employed for such a determination of the current density, the points are placed in the dashed frame.

Results Obtained. A comparison of the current densities obtained by the two methods mentioned above is presented in Fig. 6 in the form of the dependence of the current density j in the cathode spot on the copper electrode on the magnetic field B . This figure also gives the data obtained earlier by the nonstationary thermal method and the results of Kiselev [9] for the cathode spot of a cutting air arc, which have been obtained by electrical methods on a rotating sectioned copper cathode in the absence of an external magnetic field. Since Kiselev gives in [9] the radial distribution of the current density, in Fig. 6 we give the averaged values corresponding to the dimension of the zone where 95% of the current flows. The dotted curve in Fig. 6 shows the approximation of nonstationary data in the form (see [10])

$$j = \left[2.42 - 1.59 \exp\left(-\frac{B}{0.17}\right) \right] \cdot 10^9. \quad (8)$$

In approximating the stationary data on $j(B)$, we have given preference to those obtained by modeling the experimental dependences $g(I)$ with the thermal model, since they best meet the need for this model in calculations of

erosion. The above stationary data in the range of magnetic fields to 0.4 T, including Kiselev's data, can be approximated by the empirical expression

$$j = [1.3 - 2.8\exp(-141.3B) + 1.665\exp(-292B) + 3.5B] \cdot 10^9, \quad (9)$$

shown as the solid curve in Fig. 6.

From Fig. 6 it is clear that the current density obtained from the stationary data is always, in practice, higher than that determined in the nonstationary experiments. The reason may be that we have disregarded the character of motion of the arc and in all the measurements we have taken continuous motion of the spot on the electrode surface, i.e., $n = 1$ in formula (2). Thus, we obtained the apparent current density including the character of motion of the spot and not the real density. Furthermore, the duration of our stationary experiments was 10 min, whereas that of the nonstationary experiments was no longer than 2 sec. Therefore, the cathode surface in the stationary experiments was contaminated with a thicker oxide layer than the surface in the nonstationary experiments. According to the data of [11], this had to lead to a less regular motion of the spot with more frequent stops, an extension of the arc, and finally an increase in n . As follows from (2), taking that $n = 1$ for all the experiments, we obtained an obviously overstated result which differs from the real value the more significantly, the higher the n .

CONCLUSIONS

In thermal calculations of the copper cathode, we can take the linear dependence of the volt-equivalent of the heat flux in the arc spot on the magnetic field. A nonlinear exponential dependence has been obtained for the current density. The current-density values found by the nonstationary methods turn out to be lower than those obtained from the stationary experiments. The reason is, apparently, the influence of the oxide layers on the cathode surface, which have different thicknesses because of the different durations of the stationary and nonstationary experiments. To eliminate this difference and obtain more exact values one should diagnose the character of movement of the spot for a more exact determination of the time of its stay at each point of the electrode. Among the data obtained without such diagnostics, best suited for calculations of the electrodes are the results of the stationary experiments, since they include the influence of the character of motion of the spot in long-duration stationary operation of the electrode.

The authors express their thanks to A. A. do Prado for technical assistance in the work. We are also grateful to scientific funds of Brazil (CNPq, FAPESP, and FINEP) for financial support.

NOTATION

a , thermal diffusivity, $\text{m}^2 \cdot \text{sec}^{-1}$; B , magnetic induction, T; d , diameter of the spot, m; f , dimensionless parameter of fusion; F , area of the arc spot, m^2 ; g , specific mass integral erosion, $\text{kg} \cdot \text{C}^{-1}$; g_0 , specific mass microerosion, $\text{kg} \cdot \text{C}^{-1}$; h_{eff} , effective erosion enthalpy, $\text{J} \cdot \text{kg}^{-1}$; I , arc current, A; j , effective density of the current in the arc spot, $\text{A} \cdot \text{m}^{-2}$; L , step length, m; n , dimensionless length of the arc-spot step; q_0 , density of the heat flux in the spot, $\text{W} \cdot \text{m}^{-2}$; Q_0 , integral heat flux in the arc spot, W; r and s , coefficients of linear regression; R , correlation coefficient; T , temperature, K; T_0 , surface temperature of the electrode, K; T_f , fusion temperature, K; U , volt-equivalent of the heat flux, V; v , average velocity of the arc, $\text{m} \cdot \text{sec}^{-1}$; W , dimensionless erosion energy in the model of continuous motion of the spot; λ , thermal conductivity, $\text{W} \cdot \text{m}^{-1} \cdot \text{K}^{-1}$. Subscripts: f, fusion; eff, effective value.

REFERENCES

1. A. M. Esipchuk, A. Marotta, and L. I. Sharakhovskii, Erosion of a copper cathode in a nonstationary arc spot. I. Experimental investigation, *Inzh.-Fiz. Zh.*, **77**, No. 2, 106–111 (2004).
2. A. Marotta and L. I. Sharakhovskii (Sharakhovsky), Theoretical and experimental investigation of copper electrode erosion in electric arc heaters. I: The thermophysical model, *J. Phys. D: Appl. Phys.*, **29**, 2395–2403 (1996).
3. A. Marotta, L. I. Sharakhovskii, and V. N. Borisyuk, Heat transfer and plasmatron electrode erosion, *Inzh.-Fiz. Zh.*, **70**, No. 4, 551–559 (1997).

4. L. I. Sharakhovskii (Sharakhovsky), A. Marotta, and V. N. Borisyuk, A theoretical and experimental investigation of copper electrode erosion in electric arc heaters. II: Experimental determination of arc spot parameters, *J. Phys. D: Appl. Phys.*, **30**, 2018–2025 (1997).
5. L. I. Sharakhovskii (Sharakhovsky), A. Marotta, and V. N. Borisyuk, A theoretical and experimental investigation of copper electrode erosion in electric arc heaters. III: Experimental validation and prediction of erosion, *J. Phys. D: Appl. Phys.*, **30**, 2421–2430 (1997).
6. A. M. Esipchuk (Essiptchouk), A. Marotta, L. I. Sharakhovskii (Sharakhovsky), and D. A. Bubljevsky, Experimental investigation of the cathode spot parameters in magnetically driven arc, in: P. Fauchais (ed.), *Progress of Plasma Processing of Materials 2003*, Begell House, New York (2003), pp. 203–209.
7. P. Teste, T. Leblanc, and J-P. Chabrierie, Study of the arc root displacement and three-dimensional modelling of the phenomena occurring in a hollow cathode submitted to an electric moving arc, *J. Phys. D: Appl. Phys.*, **28**, 888–898 (1995).
8. A. M. Esipchuk, A. Marotta, and L. I. Sharakhovskii, Magnetic-field effect on heat transfer within a cathode arc spot, *Inzh.-Fiz. Zh.*, **73**, No. 6, 1245–1254 (2000).
9. Yu. Ya. Kiselev and V. K. Pogora, Radial current-density distribution in the main spots in a plasma cutting arc, *Inzh.-Fiz. Zh.*, **53**, No. 2, 284–289 (1987).
10. A. M. Esipchuk, A. Marotta, and L. I. Sharakhovskii, Experimental investigation of the current density and the heat-flux density in the cathode arc spot, *Inzh.-Fiz. Zh.*, **74**, No. 3, 198–206 (2001).
11. R. N. Szente, R. J. Munz, and M. G. Drouet, The influence of the cathode surface on the movement of a magnetically driven electric arc, *J. Phys. D: Appl. Phys.*, **23**, 1193–1200 (1990).